Nuclear Instruments and Methods in Physics Research A 484 (2002) 494–502

NUCLEAR INSTRUMENTS & METHODS IN PHYSICS RESEARCH Section A

www.elsevier.com/locate/nima

Neutron-induced Single Event Upset on the RPC front-end chips for the CMS experiment

M. Abbrescia[a], A. Colaleo[a], G. Iaselli[a], F. Loddo[a], M. Maggi[a], B. Marangelli[a], S. Natali[a], S. Nuzzo[a], G. Pugliese[a], A. Ranieri[a], F. Romano[a], S. Altieri[b], G. Belli[b], G. Bruno[b], R. Guida[b], M. Merlo[b], S.P. Ratti[b], C. Riccardi[b], P. Torre[b], P. Vitulo[b,*], A. de Bari[c], S. Manera[c]

[a] *Dipartimento Interateneo di Fisica and INFN Sezione di Bari, via Amendola 173, I-70126 Bari, Italy*

[b] *Dipartimento di Fisica Nucleare e Teorica, Università di Pavia and INFN Sezione di Pavia, via Bassi 6, I-27100 Pavia, Italy*

[c] *Centro Interdipartimentale "L.E.N.A" Laboratorio di Energia Nucleare Applicata, Pavia, via Aselli, 41, I-27100 Pavia, Italy*

Received 28 May 2001; received in revised form 2 August 2001; accepted 8 August 2001

Abstract

Neutrons from a reactor and from a cyclotron have been used to characterise the CMS Resistive Plate Chambers (RPCs) front-end chip to neutron-induced damaging events. Single Event Upset (SEU) cross-sections have been measured up to 60 MeV for different chip thresholds. Tests at a reactor were done with an integrated fast ($E_n > 3$ MeV) neutron fluence of 1.7×10^{10} cm^{-2} and a thermal neutron fluence of 9.5×10^{11} cm^{-2}. High-energy neutrons from a cyclotron were used up to a fluence of 10^{12} cm^{-2}. Data indicate the existence of a chip SEU sensitivity already at thermal energy and a saturated SEU cross-section from 3 to 60 MeV. Values of the SEU cross-sections from the thermal run well agree with those obtained by another CMS group that uses the same technology (0.8 μm BiCMOS) though with different architecture. Cross-sections obtained with fast neutrons (from 3 MeV to about 10 MeV) are consistently higher by one order of magnitude compared to the thermal one. The average time between consecutive SEU events in each chip of the CMS barrel RPCs can be estimated to be 1 h. © 2002 Elsevier Science B.V. All rights reserved.

1. Introduction

Data corruption of electronic devices under irradiation has been first studied in connection with aircraft electronics failures [1–4] due to the interactions of cosmic rays producing Single Event Effects (SEE) into the semiconductor nodes of digital memories. SEE are radiation-induced damaging events that can give an erroneous behaviour or a failure of an electronic device under irradiation. The damage caused by the entering radiation can be of static nature, as in the case of digital memory bit flipping creation, or of transient nature, as in the case of produced charge carriers that propagate through the device, or even of disruptive nature when the energy of the

*Corresponding author. Tel.: +39-382-507-633; fax: +39-382-526-938.

E-mail address: paolo.vitulo@pv.infn.it (P. Vitulo).

0168-9002/02/$ - see front matter © 2002 Elsevier Science B.V. All rights reserved.
PII: S0168-9002(01)01967-2

incoming particle is high enough to produce burnouts or gate ruptures. The vulnerable part of a chip seems to be the digital circuit and so the available data, both in simulations and measurements, are essentially concentrated on digital devices like SRAM, DRAM, FLASH memories or DSP and PLUs.

The neutrons and charged hadrons environment that will be created during the running time around the future experiments at the Large Hadron Collider (LHC), represents a potential SEE source for the detectors front-end and slow control electronics. Several authors [5–8] have already started the investigation of the phenomenon.

In the following, we will concentrate on transient effects — Single Event Upsets (SEU) — and results will be shown for the case in which neutrons generate a voltage shift at a node inside the device under test with the effect of inducing voltage fluctuations of sufficient amplitude to simulate true output signals. When disturbances exceed a fixed threshold, the pulses generated and collected by the following electronics can be counted, for example, by a scaler.

The tested electronics is the Resistive Plate Chambers (RPCs) front-end chip (FEC in the following) of the CMS experiment [9].

RPCs will operate as muon detectors in the barrel and forward regions of the CMS experiment. The expected radiation environment in the muon barrel region is mainly composed of gammas and neutrons. The neutrons are generated directly from the hadronic interactions in the calorimetries or from the interaction of the primary proton beam with the beam pipe and/or the beam collimators located externally just before the experiment end-caps. The gamma radiation is mainly due to neutron capture in the surrounding material. For this reason a background made of gammas and neutrons will enfold each detector of the experiment.

In the muon barrel, the maximum radiation energy is expected at several MeV for gammas and up to 100 MeV for neutrons. Moreover, simulations show that the total expected radiation dose (gammas plus neutrons) absorbed after 10 years of operation will be, in the worst case of the CMS end-cap regions, about 30 Gy. A dose smaller by an order of magnitude is expected in the muon barrel and the foreseen neutron fluence might not be high enough to generate a relevant bulk damage of the chips, at least for neutron energy of 20 MeV.

Moreover, measurements show that disruptive events have a very low cross-section. In the muon barrel, neutron and gamma flux is foreseen to be quite low (some hundreds ($cm^{-2}\,s^{-1}$)). Nevertheless, the high number of chips in the detectors (about 10,000 in the barrel RPCs for example) can make the total SEU rate of the order of some Hz.

Neutron sources were thus used to characterise the RPC front-end chip to neutron-induced damaging effects.

2. Neutron sources

Neutron sources were available at a nuclear reactor and at a cyclotron facility. We used the Laboratorio Energia Nucleare Applicata (LENA of the University of Pavia) 250 kW Triga Mark II Reactor to irradiate the FECs with neutrons ranging from thermal energies up to about 10 MeV, while the Louvain-la-Neuve Cyclotron of the Catholic University of Louvain (UCL) has been used to obtain neutrons of energy up to 60 MeV.

The Triga Mark II is a water-cooled and water-moderated reactor. At full power (250 kW) the available flux along the core axis is 5×10^{13} $cm^{-2}\,s^{-1}$. Several extraction channels located around the cylindrical arrangement of the core are available as irradiation facilities. Our equipment was located at the end of the thermal column where an irradiation channel ends in a rectangular shaped window of 20×40 cm and where a Boral window (aluminium and boron carbide particles between two layers of aluminium cladding) can be inserted. Inside the column, the spectrum is mainly thermal ($10^9\,cm^{-2}\,s^{-1}$) while downstream the window the thermal component of the spectrum is significantly reduced, due to (n,α) reactions on boron. The fast neutron flux ($E_n > 3$ MeV) at the test location was measured using targets activation and resulted to be $9.4 \times 10^4\,cm^{-2}\,s^{-1}$. The analysis of other activated targets located close to the chips revealed beam uniformity within 10%.

The Cyclotron was used to obtain high-energy neutrons. The beam is permanently used for therapy purposes and neutrons are produced by bombarding a 10 mm thick Be target with 50 MeV deuterons or a 17 mm thick Be target with 65 MeV protons [10]. Neutron flux estimate was based on dose measurements done by other groups [11]. For our test, protons were used for neutron production and a yield of 2.72×10^6 n μC^{-1} cm^{-2} was estimated at the test location. Through the monitoring of the proton beam current, we were able to measure the total neutron flux. With a proton current of 15 μA, a flux of 4×10^7 n cm^{-2} s^{-1} was achieved.

2.1. Fast neutrons at the reactor

The evaluation of the SEU rate requires the knowledge of the neutron flux at the test location. Several Ni targets were exposed to the neutron beam and their saturation activity A_s calculated counting, by a germanium detector, the ^{58}Co gamma emission at 811 keV produced in the $^{58}Ni(n,p)^{58}Co$ reactions. Irradiating time, gamma counting time and time lag between the end of the irradiation and the beginning of the counting were properly accounted for the final evaluation of A_s. The flux F was calculated by means of the

$$\Phi = \frac{A_s}{\sigma n N_a I_s} \tag{1}$$

where n is the number of Ni moles, N_a the Avogadro number, I_s the ^{58}Ni isotopic abundance and σ the effective cross-section, being

$$\sigma = \frac{\int_{3\ \mathrm{MeV}}^{10\ \mathrm{MeV}} \sigma(E)\Phi(E)\,\mathrm{d}E}{\int_{3\ \mathrm{MeV}}^{10\ \mathrm{MeV}} \Phi(E)\,\mathrm{d}E}. \tag{2}$$

The lower value of the integrals has been set to 3 MeV where the $^{58}Ni(n,p)^{58}Co$ reactions start to be effective. In Eq. (2) the neutron energy spectrum $F(E)$ at the test location was supplied by a simulation program based on the MCNP-4b Monte Carlo code [12] which fully simulated the reactor geometry and all the materials around the neutron beam.

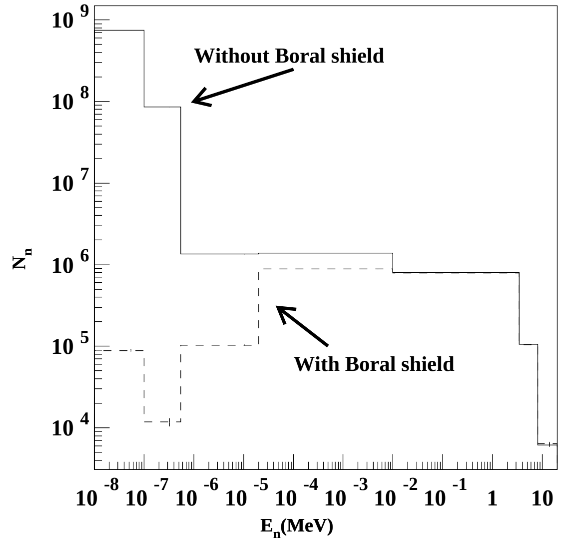

Fig. 1. Simulated neutron spectrum upstream and downstream the Boral shield; the Boral window insertion allows operating with a reduced thermal flux.

The source spectrum was assumed to be a Watt fission spectrum. Fig. 1 shows the simulated neutron spectrum immediately upstream and immediately downstream the Boral window. A significant fraction of the thermal neutrons, fully contained in the first bin of the histogram, is removed from the available spectrum by the insertion of the Boral shield.

2.2. Thermal neutrons at the reactor

In a specific run with the Boral window opened, Cu targets were used to measure the neutron thermal component. In this case the 511 keV gamma emission from ^{64}Cu produced in the $^{63}Cu(n,\gamma)^{64}Cu$ reactions was counted. The formula used for the flux estimate is Eq. (1) with σ (4.5 b) being the ^{63}Cu thermal cross-section at 0.025 eV and I_s the ^{63}Cu isotopic abundance, leading to a flux of 4.4×10^8 n cm^{-2} s^{-1}.

2.3. Neutrons from the cyclotron

Fig. 2 shows the neutron energy spectrum obtained from [13] at the Cyclotron test location.

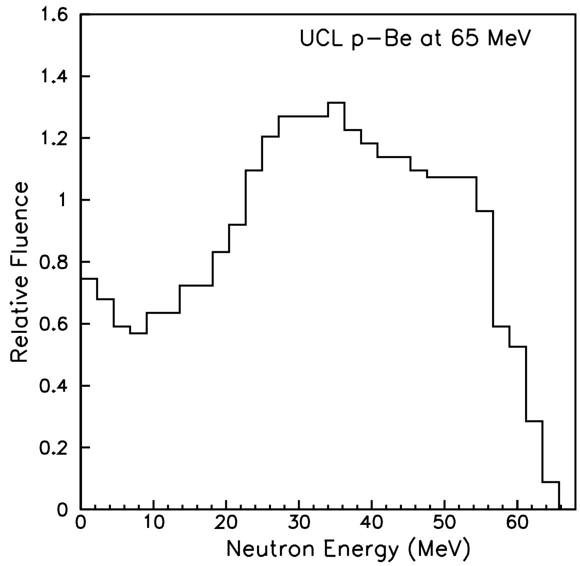

Fig. 2. Energy spectrum of the neutron beam from the Cyclotron.

The portion of the area subtended by the histogram for energies less than 10 MeV is about 10% of the total. For this reason, SEU data were interpreted as due mainly to the higher part of the spectrum.

3. Test setup

A RPC front-end board (FEB in the following) contains two 8 channels chips (FECs) and two Digital to Analogue Converters (DACs) to set, store and distribute threshold to the FEC. The input threshold fixes the equivalent charge threshold value to the chips. Two front-end boards were irradiated with unconnected inputs. The Low Voltage Differential Signals (LVDS) outputs, shaped at 80 ns, were sent to an LVDS-ECL level translator module through a twisted pair cable connection. The module provided also two NIM level outputs for the OR of 8 channels (OR8 in the following) from each chip. The input threshold was changed during the tests from 50 to 150 mV. At the reactor, the boards were positioned 15 cm far from the Boral window and 5 Ni targets were placed directly onto the electronics to detect the actual fast neutron flux. A PC, in communication with a VME crate via a VME-MXI-2 interface by National Instruments, performed the main control. The outputs from a LVDS-ECL translator fed a VME 16 channels CAEN Scaler in two different configurations so that the 16 channels from one board or the four OR8 from the two FEBs could be read separately at once. The Scaler was monitored by a LabView interface written on Windows NT platform and data were stored in a database in Microsoft Excel format.

At each run, we could set the threshold value separately on each board and change the time interval between two sequential acquisitions. At the Cyclotron, two front-end boards were positioned at the multileaf collimator output of the Louvain fast neutron therapy facility, 183 cm far from the Be target.

Reading and conversion of the signals were made in the usual way by feeding a LVDS-ECL receiver. The measurement of the SEU rate was made through the counting of each chip OR8. The error flag of a latch-up protection circuit, mounted on board for this test, was monitored to detect Single Event Latch-up failures. The preset threshold voltage value was checked every 30 s by reading the DACs bits content.

4. Results

In the literature, a device SEU sensitivity is usually expressed in terms of cross-section. It can be estimated either by the ratio of the measured SEU rate (s^{-1}) to the radiation flux ($cm^{-2}\,s^{-1}$) seen by the device under test or through the slope of the curve obtained by plotting the number of SEU events as a function of the particle fluence (cm^{-2}).

It should be noted that with this approach the value of the mentioned cross-section does represent the product of the number of material targets times the microscopic cross-section for the particular process. Since a SEU event is also correlated with the amount of the deposited charge close to a sensitive node of the chip, we expect a different behaviour of the device as a function of the threshold.

4.1. Thermal neutron results

Low-energy neutron SEU sensitivity has been attributed to the presence of the boron as doping agent in the manufacturing of the integrated circuits. In particular, the high neutron capture cross-section of the isotope ^{10}B can increase the probability of occurrence of SEU events for thermal neutrons and should be proportional to the boron concentration close to the sensitive nodes. Moreover, simulations of digital devices with different boron concentrations [14] show that a uniform boron concentration as high as 10^{17} cm^{-3} can only account for a SEU probability that is 3 orders of magnitude lower than what is expected for higher neutron energy, the value decreasing several orders of magnitude as the deposited energy increases towards 1 MeV. According to the manufacturer, our chips were natural boron doped to a concentration of 2×10^{16} cm^{-3} at the p-well, for a depth of 1.5 μm. This concentration drops exponentially in the following 3.5 μm to reach the p-substrate (525 μm depth) concentration of 7×10^{14} cm^{-3}. According to these values and to the results of Ref. [14] we would expect a very low SEU sensitivity in the thermal neutron energies. To verify these hypotheses a special run with thermal neutrons was performed in which the Boral window at the end of the reactor thermal column was opened. During the run, with a thermal flux of 4.4×10^8 n cm^{-2} s^{-1}, data were accumulated for different values of the chips thresholds.

A neutron fluences of 8.15×10^{11}, 9.5×10^{11}, 9.5×10^{11} and 4.1×10^{11} cm^{-2} for thresholds of 50, 75, 100 and 150 mV were respectively integrated. Fig. 3 shows for example the number of SEU events in one chip as a function of the neutron fluence for different thresholds. A linear fit is superimposed and the value of the slope directly gives the value σ_{SEU} of the cross-section (e.g. 7.35×10^{-8} cm^2 at 50 mV).

The same behaviour was verified for all others chips. Data show that, for our chips, neutron-

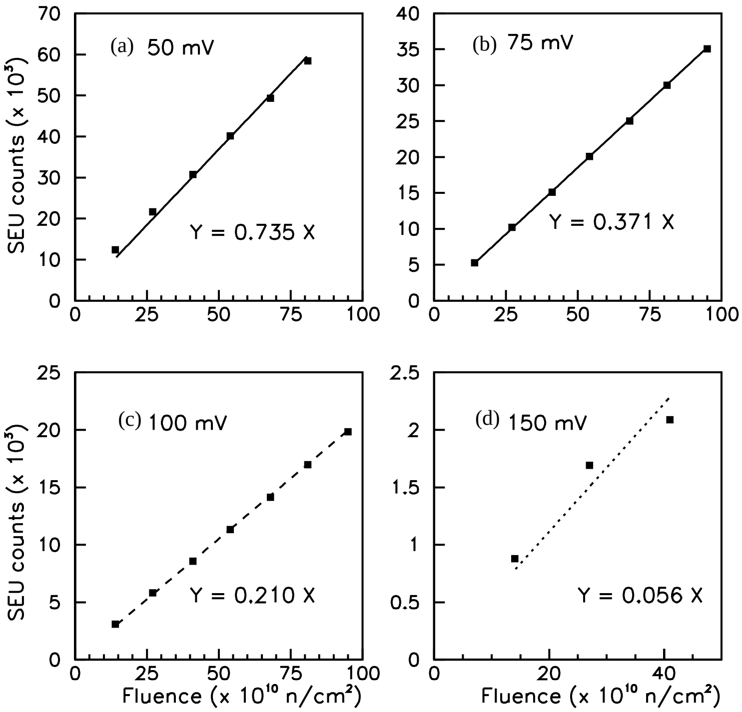

Fig. 3. SEU cross-section evaluation, for the thermal run. SEU events are plotted as a function of the measured neutron fluence for a chip threshold of (a) 50, (b) 75, (c) 100, and (d) 150 mV.

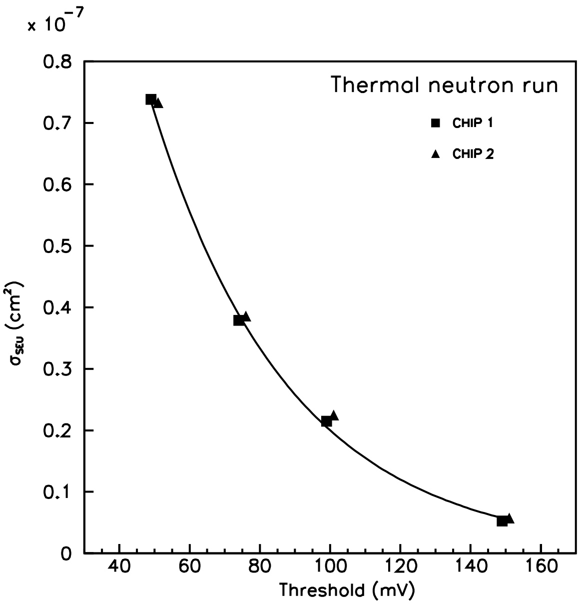

Fig. 4. SEU cross-section as a function of the chips threshold for the thermal run. The dashed line represents an exponential curve, superimposed to guide the eyes.

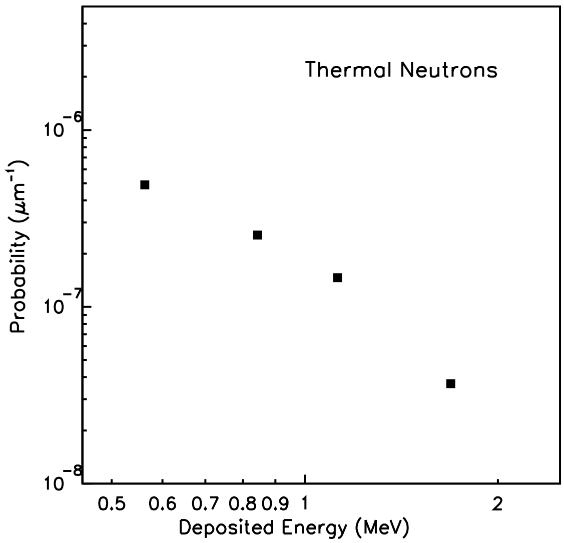

Fig. 5. SEU Integral Probability evaluated for our chips assuming a sensitive volume SV of 1.5×10^{-5} cm^3. The curve shows the probability to have a SEU event in the volume SV for a deposited energy greater or equal to the one evaluated.

induced SEU events are effective already at thermal energies. Values of the cross-sections are of the same order of those obtained by the CMS Drift Tubes group [6] that uses the same technology (0.8 μm BiCMOS) though with different architecture. Fig. 4 summarises the results for two chips in a plot of σ_{SEU} as a function of the imposed threshold value. An exponential line is superimposed to guide the eye. The average minimum energy E_T deposited by neutrons into a chip can be calculated from the voltage threshold V_{th} set at the front-end and from the chip sensitivity S(2 mV/fC) as

$$E_T = (V_{\mathrm{th}}/S \times q_{\mathrm{e}}) \times E_{\mathrm{ion}} \quad (3)$$

where q_{e} is the electron charge and E_{ion} the assumed silicon ionisation energy (3.6 eV). In our case, the average minimum deposited energies in MeV were 0.56, 0.84, 1.13 and 1.69 for thresholds of 50, 75, 100 and 150 mV, respectively. Several authors [15,16] refer their calculations on SEU probability to the knowledge of the sensitive volume SV into which a neutron interacts. Usually, this volume is a reasonable guess of the sensitive region of the chip under test. By considering, for our chips, a sensitive area of 10 mm^2 and a sensitive depth of 1.5 μm an effective volume SV of 1.5×10^{-5} cm^3 is estimated as a SEU source. The average integrated probability that a neutron, travelling for a micron inside such a sensitive volume would produce a SEU event, is given by the ratio of the measured SEU cross-section to SV. Fig. 5 shows this calculated integrated probability as a function of the minimum deposited energy previously calculated. Data show that a variation by a factor three in the deposited energy corresponds to a variation of about one order of magnitude in the probability of SEU occurrence.

4.2. Fast neutron results at the reactor

The run with fast neutrons was done with the Boral window inserted and lasted about 52 h during which thresholds were changed. A fast neutron fluence of 1.7×10^{10} cm^{-2} was accumulated. Despite the insertion of the Boral window, a fraction α of the spectrum in the thermal region might survive and might add to the fast SEU rate. A correction to the measured fast cross-section σ_f^m has been taken into account according to the equation

$$\sigma_f^m = (R_1 + R_2)/(\Phi_1 + \alpha\Phi_2) \quad (4)$$

being R_1, R_2, Φ_1, Φ_2, respectively the true SEU rate due to fast neutrons, the true SEU rate due to the survived thermal neutrons, the measured fast neutron flux and the measured thermal neutron flux. An equivalent relation,

$$\sigma_t^m = (R_1 + R_2/\alpha)/(\Phi_1 + \Phi_2) \quad (5)$$

applies for the thermal run and together with the previous equation, allows to obtain the true rates R_1 and R_2 as well as the corresponding corrected SEU cross-sections $\sigma_1 = R_1/\Phi_1$ and $\sigma_2 = R_2/\alpha\Phi_2$, being R_2/α the rate due to all the thermal neutrons. Since the Boral window does not alter significantly the fast spectrum, the same fast rate R_1 has been considered in both the previous equations. The value $\alpha = 2.5 \times 10^{-4}$ has been provided by the simulation. The ratio σ_1/σ_2 ranges from 9.3% to 11.4% according to the different thresholds. Unlike the thermal run, where corrections to the cross-section are negligible, for the fast neutrons run the corrected cross-sections are about a factor 2 higher.

Fig. 6 summarises the corrected SEU cross-section for fast neutrons as a function of the imposed threshold for three chips. A change of a factor three in the threshold — from 50 to 150 mV — corresponds to a change of a factor 10 in the cross-section.

Fig. 7 shows the integrated probability, as previously defined, as a function of the minimum deposited energy calculated for the fast neutrons (full squares); corresponding data for the thermal run—Fig. 5—have been superimposed for comparison (full triangles). The ratio of the two curves is about a factor 10.

4.3. Louvain fast neutrons results

The run at the Louvain Cyclotron lasted 6 h during which a neutron fluence of 10^{12} cm^{-2} was accumulated. Unfortunately, the environment noise conditions allowed running only at high

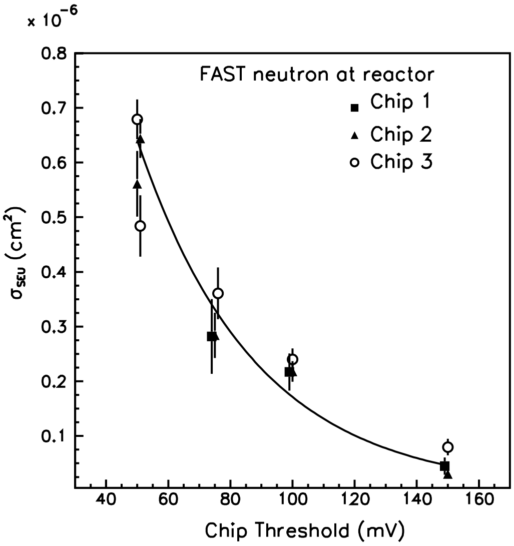

Fig. 6. Corrected SEU cross-section as a function of the threshold for three different chips. Data refer to the fast neutron run where a total fluence of 1.7×10^{10} cm^{-2} was accumulated. An exponential line has been superimposed to guide the eye.

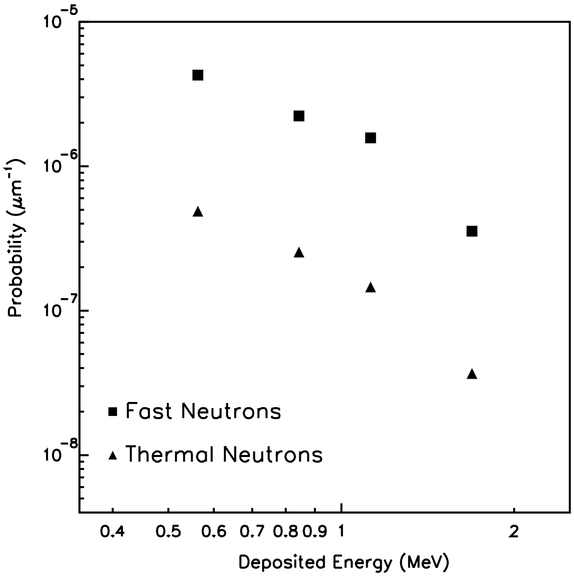

Fig. 7. SEU Integrated probability, corrected for the thermal neutron contribution, as a function of the minimum deposited energy. Full squares correspond to the fast neutron yield while the thermal contribution, from Fig. 5, has been superimposed as comparison (full triangles).

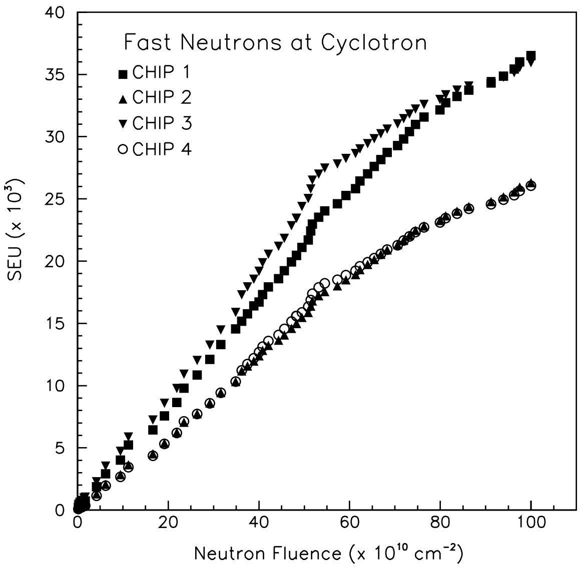

Fig. 8. SEU events as a function of the neutron fluence for 4 chips. Neutrons were obtained from the Louvain-la-Neuve Cyclotron as described in the text. Values of the cross-sections were equivalent to those obtained in the fast neutron run at the reactor for the same threshold (150 mV).

thresholds. Useful data for comparison with lower energy neutrons will be shown for a threshold of 150 mV. Fig. 8 shows the recorded SEU events as a function of the neutrons fluence for four chips. A linear behaviour is noticed and above 5×10^{11} cm^{-2} a change in the slope seems to appear. A linear fit to the data up to this fluence returned SEU cross-sections of 4.79×10^{-8}, 4.21×10^{-8}, 3.14×10^{-8} and 3.07×10^{-8} cm^2, respectively, similar to those obtained in the fast neutron run at the reactor for the same thresholds. No latch-up events were observed during the run. The assumption made in Section 2.3 that all the SEU events measured at the Cyclotron might be attributed to the higher part of the spectrum seems reasonable. An inspection of Fig. 2 reveals that the neutron energy spectrum in the range 20–60 MeV is almost flat and since the cross-section values are of the same order of those obtained at the reactor fast run, we might conclude that there exists an evidence for the saturation of the SEU cross-section in the energy range 3–60 MeV. Additional data at resolved neutron energies would be more conclusive about this point.

5. Final remarks

Two neutron irradiation facilities have been used to characterise the Resistive Plate Chambers front-end chips of the CMS experiment to neutron-induced SEUs. As expected, neutron-induced SEU events are effective already at thermal energies and the cross-section values in this energy range agree with those obtained by the CMS Drift Tubes group that used the same technology (0.8 μm BiCMOS) with a different architecture. As already mentioned, the SEU cross-section varies with the imposed threshold, indicating that a minimum deposited charge inside a sensitive volume is needed to trigger the entire SEU process. In our tests, we varied the chips threshold from 50 to 150 mV, equivalent to an input charge range from 25 to 75 fC. For higher neutrons energies (from 3 to about 10 MeV) the cross-section is one order of magnitude higher than the thermal one. This result is one order of magnitude higher than those obtained by the CMS drift tubes group [6] for similar neutron energies; this is not so surprising since in the literature very large variations (over 3 orders of magnitude) can be found for similar devices. Fig. 9 summarises the results of the tests made at different energies in terms of measured SEU cross-section and for the same threshold (150 mV). Data seem to provide evidence for a saturation of the cross-section from 3 to about 60 MeV.

It is interesting to calculate the average mean time between SEU events per chip in the CMS barrel by assuming a uniform distribution of the flux and a saturation SEU cross-section, from Fig. 6, of 6×10^{-7} cm^2 (corresponding to 50 mV threshold). In a conservative estimate, we assume an average total flux of 400 n cm^{-2} s^{-1} from thermal energies up to 100 MeV. The corresponding average time between SEU events in each RPC chip would then be about 1 h. Concerning the level of absorbed doses, simulation data anticipate a total value of the order of 1 Gy in 10 years of running in all regions of the experiment. In our

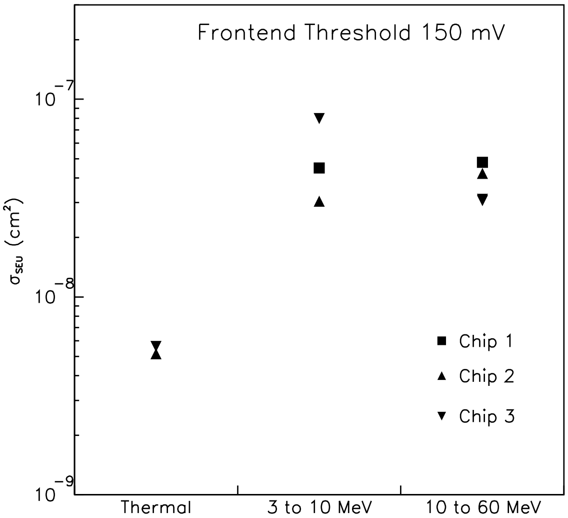

Fig. 9. Measured SEU cross-section, for three chips as obtained in the three tests. Data are compared for a threshold of 150 mV.

tests dose levels were well beyond this prediction. For example, we accumulated 40 Gy at the Louvain-la-Neuve Cyclotron and a dose rate of 1 Gy/h has been measured at the Pavia reactor. It should be pointed out, however that at the Pavia reactor much of the dose in the fast run was due to gammas produced through capture reactions into the Boral window. Results from the test at higher neutron energies, indicate a change in the cross-section after a neutron fluence of about 5×10^{11} cm^{-2} (see Fig. 8). The reason for that is still unclear. Bulk damage might be the reason; however, the chips have been tested after the run and showed no degradation both in their timing characteristics and in the drawn current. The estimated threshold LET(MeV cm^2 mg^{-1}) during these irradiations can be calculated through the mean threshold energy E_T (from Section 4.1) to be LET $= E_T/(\rho_{Si} z) = 4.9$ MeV cm^2 mg^{-1}, being ρ_{Si} the Silicon density and z the estimated sensitive depth (1.5 μm). Characterisation of the chip with high-energy ions would explore the possibility of its use in other applications.

Acknowledgements

We would like to acknowledge the support given by the Pavia and Bari technical staff during the arrangement of the tests. We also thank the Triga Mark II operators for providing us the required hours of continuously running and the personnel of the Cyclotron at Louvain-la-Neuve, for their precious collaboration.

References

[1] J. Olsen, et al., IEEE Trans. Nucl. Sci. NS-40 (1993) 74.
[2] A. Taber, et al., IEEE Trans. Nucl. Sci. NS-40 (1993) 120.
[3] C.A. Gosset, et al., IEEE Trans. Nucl. Sci. NS-40 (1993) 1845.
[4] E. Normand, et al., IEEE Trans. Nucl. Sci. NS-40 (1993) 1484.
[5] F. Faccio, et al., CERN CMS Note 1998/054.
[6] S. Agosteo, et al., CERN CMS Note 2000/024.
[7] F. Faccio, et al., CERN/LHCC/99-33, Proceedings of the Fifth Workshop on Electronics for LHC Experiments, Snowmass, CO, September 20–24 1999, 2000, pp. 571.
[8] J. Fulcher, et al., CERN/LHCC/99-33, Proceedings of the Sixth Workshop on Electronics for LHC Experiments, Cracow, Poland, September 11–15 2000, p. 260.
[9] F. Loddo, et al., Nucl. Instr. and Meth. A 456 (2000) 143, Proc. of the Fifth Workshop on Resistive Plate Chambers and related detectors, Bari, Italy, October 28–29 1999.
[10] S. Vynckier, et al., Phys. Med. Biol. 28 (6) (1983) 685.
[11] J.M. Denis, et al., Bull Cancer/Radiother. 83 (Suppl. 1) (1996) 160.
[12] J.F. Briestmeister (Ed.), A General Monte Carlo N-particle Transport code, Los Alamos National Laboratories Report LA-12625-M Version 4B, Los Alamos, New Mexico, 1997.
[13] Nuclear data for neutron and proton radiotherapy and for radiation protection, ICRU Report 63 (1999) 14.
[14] M. Hutinen, F. Faccio, Nucl. Instr. and Meth. A 450 (2000) 155.
[15] C. Vial, et al., IEEE Trans. Nucl. Sci. NS-45 (6) (1998) 2915.
[16] K. Johansson, et al., IEEE Trans. Nucl. Sci. NS-45 (6) (1998) 2519.